

Enterprise Biology Software Project

PO Box 292
Medina, Washington 98039-0292

Enterprisebiology.com
playingcomplexitygames.com

ANNUAL REPORT

2017

The report postulates that - within and across species - the same genetic information (DNA) produces the same phenotypic parts. To test this postulate, we apply the same rules biology uses in defining a phenotype to predict relationships of structure to function within and across species.

Enterprise Biology Software: XVIII. Research (2017)

ROBERT P. BOLENDER

Enterprise Biology Software Project, P.O. Box 292, Medina, WA 98039-0292, USA
(enterprisebiology.com)

SUMMARY

Given the encouraging results reported last year for membrane surface areas, we now have the incentive to look for specific mathematical links between morphology and biochemistry. We also know from textbooks on molecular cell biology (Alberts et al., 2014; Lodish et al., 2016) that genomes across animal species display remarkable similarities. In fact, many biological parts in different animals display what appear to be identical DNA sequences. This raises an interesting question. If different animals share the same DNA coding for given part, do such parts also share the same phenotype? The report this year attempts to answer this question by making two assumptions. The first of these assumes that the postulates of deDuve (biochemical homogeneity and single location) are correct, while the second one assumes that equations based on these postulates have the power to predict experimental outcomes. Since we already know from an earlier report (2003) that predicting outcomes in biology requires equations with $R^2 = 1$, our task becomes one of identifying relationships of structure to function using equations capable of fulfilling the requirements of prediction and the homogeneity postulates (deDuve, 1974). If successful, we will have an answer to our question and perhaps the beginnings of a new strategy for shuttling data back and forth between the phenome and the genome. As the story unfolds, we will have to decide –repeatedly - how to access a highly organized and complex biology using data taken from a highly eclectic and disconnected literature. Consequently, prediction often comes to our rescue. This will include predicting morphology from biochemistry, biochemistry from morphology, morphology from morphology, and biochemistry from biochemistry. Since the report consists largely of reworking the original data of published studies, calculation worksheets are included in the Appendix as Excel (Microsoft, Redmond, WA) and Mathematica (Wolfram Research, Champaign, IL) files. The report in its entirety is available online (playingcomplexitygames.com).

INTRODUCTION

A postulate is a statement assumed to be true without proof - existing as a self-evident, basic principle.

In this report, we consider two such postulates. They come from the relationship of structure and function and serve to connect cell to molecular biology. The story of these

postulates will be told with equations derived from biology by way of the biology literature.

Let's begin. If the relationship of structure (S) to function (F) is linear, then the slope (m) of the curve defines this relationship as:

$$F = mS \quad (1)$$

$$S = F/m \quad (2)$$

where $m = \Delta y/\Delta x$.

Notice that the slope defines each rule as a ratio ($m = F/S$ or $m = S/F$). By becoming familiar with such rules, we can use them to predict data and patterns that don't currently exist in the literature. In effect, prediction becomes a new problem-solving tool.

The Strategy

The report introduces the **postulate of biological homogeneity**, which states that biological parts derived from the same instructions in the genome display the same relationships of structure to function in the phenome. In effect, this means that the equations defining a biological part, such as the liver, apply equally well to livers of similar and different animal species – when they carry the same set of genetic instructions. Before we can test this new postulate, however, we must first verify the two biochemical postulates of deDuve (1964, 1974), which serve to define the relationship of structure to function in biology.

The **postulate of biochemical homogeneity** states that members of a given population have the same biochemical composition, whereas the **postulate of single location** assumes that each constituent [marker enzyme] is restricted to a single intracellular site. In short, enzymes (biochemical constituents) are uniformly distributed at unique cellular locations (morphological components).

For convenience, we will pursue an approach largely unfamiliar in biology, wherein published experimental data will be fitted to equations displaying $R^2s = 1$ and, in turn, used to predict outcomes (equations) with similar R^2s . Why $R^2s = 1$? With such equations, structure and function become interchangeable wherein one can predict the other.

To this end, we will direct a series of questions to data sets coming from several different publications. For example, does biochemical homogeneity exist in the hepatocytes of rat livers? Are marker enzymes restricted to a single cellular location? Do livers display biological homogeneity? Why is prediction indispensable? What does it take to play a win-win game with the biology literature?

The Process

Several years ago, we attempted to confirm the postulates of deDuve by combining morphology (stereology, freeze-fracture, and cytochemistry) with biochemistry (analytical fractionation and enzymology) – (Blouin et al., 1977; Bolender, et al., 1978; Weibel and Paumgartner, 1978; Losa et al., 1978; Bolender, et al., 1980). By calculating recoveries, we could show that both morphology and biochemistry were largely conserved. Instead of confirming biochemical homogeneity, however, the data suggested biochemical heterogeneity. Moreover, the postulate of unique location was left untested.

But why try again? The difference between then and now is that our prospects for success are much improved. We now have three new clues - one from the 2003 report (prediction requires $R^2 = 1$), one from the 2016 report (reproducibility exists within and across cells and animals), and one from molecular biology (biological parts - e.g., cells and organs - can share remarkably similar genetic coding within and across species). Since it seems likely that biochemical homogeneity exists (based on the genetic evidence alone) and since we have a strategy for finding it ($R^2 = 1$), we can approach the homogeneity problem as a mathematical puzzle. Moreover, we can add a measure of confidence by conceding at the outset that our solutions do little more than mimic solutions that already exist in biology. This strategy,

which consists of creating parallel complexities, always seems to work provided we get biology's approval. Prediction and reproducibility signal such approval.

Our first job becomes one of figuring out how to set up the problem such that we can use published data to solve for biochemical homogeneity and unique location. If we start with the first paper of the previous attempt (Bolender et al., 1978), we have morphological and biochemical data sets derived from intact tissue and biochemical fractions. The paper reported individual animal data for the morphology, but just averages (mean values) for the biochemistry. Consequently, the available data set will determine our approach to solving the first problem (biochemical homogeneity). We know that the morphological data will supply the three data points needed to write a linear equation, but how do we get the three corresponding data points from just one biochemical value?

METHODS AND RESULTS

The Enterprise Biology Package

The 2017 package includes the yearly report and related worksheets (Appendix).

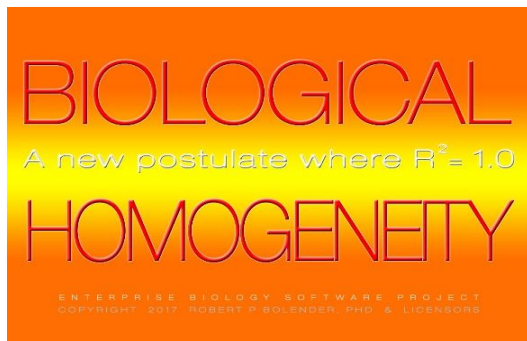


Figure 1 The EBS package for 2017 includes the yearly report with a focus on postulates central to cell and molecular biology.

Overview

The report revisits the data of several published studies with the goal of extracting new information from old data. This will be done within the framework of a new postulate (**biological homogeneity**), one that assumes a one to one relationship exists between the genome and phenome. We will argue that if the livers of two animals represent the downstream product of the same genetic information, then these livers can be expected to share the same set of rules – independent of the species in which they live.

Biochemical Homogeneity

We begin by exploring the deDuve's postulate of biochemical homogeneity, the results of which will allow us to make biochemical and morphological predictions. In turn, we will use these predictions to test the new postulate of biological homogeneity.

Paper 1 (original data): By combining morphological and biochemical data within the framework of analytical fractionation (deDuve, 1964, 1974), it was possible to show by calculating recoveries that morphological and biochemical data were conserved similarly (Bolender, et al., 1978). Such a finding represented an essential first step in confirming the postulates of deDuve.

Paper 1 (data reworked): If these biochemical postulates are correct, then the reworked data should fit a curve with an $R^2 = 1$. Morphology should follow biochemistry and vice versa. In effect, the relationship of structure to function becomes the set of biological rules given at the outset as Equations 1 and 2.

Consider the first problem we have to solve. If we have individual animal estimates for the surface areas of the endoplasmic reticulum (ER)

and a single, mean value for its marker enzyme glucose-6-phosphatase (G-6-Pase), how do we translate these data into curve with an $R^2 = 1$? These data are shown in Table 1.

Table 1 Membrane surface area (ER) in the intact tissue is juxtaposed to the activity of an er marker enzyme (G-6-Pase). Both are derived from the rat liver.

G-6-PASE	membrane	enzyme	
ER	surface	activity	
	m ² /g liver	U/g liver	
	tissue	homogenate	
	er	g-6-pase	
animal 1	er-1	4.870	27.421
animal 2	er-2	4.310	27.421
animal 3	er-3	4.620	27.421

As presented in Table 1, the published data cannot give us a curve with an $R^2 = 1$ because they do not yet conform to the homogeneity postulate of deDuve (1964). A given amount of membrane surface area (ER) does not carry the same amount of enzyme activity, which in Table 1 is given as an average value [(27.421 units of enzyme activity (U/g))].

An equation will help. It shows how we can reallocate the average enzyme activity in proportion to the amount of er membrane in each animal:

$$4.87x + 4.31x + 4.62x = 27.421, \quad (3)$$

where $x = 1.9871$, and

$$4.87 * x = 9.677$$

$$4.31 * x = 8.564$$

$$4.62 * x = 9.180.$$

When the membrane surfaces and enzyme activities are related proportionately in accord with the postulate of biochemical homogeneity, we obtain the required results (Table 2). For further details, see the calculation worksheet in the Appendix (playingcomplexitygames.com; Report 2017).

Table 2 The experimental data now conform to the postulate of biochemical homogeneity.

G-6-PASE	membrane	enzyme	
ER	surface	activity	
	m ² /g liver	U/g liver	
	tissue	homogenate	
	er	g-6-pase	
animal 1	er-1	4.870	29.031
animal 2	er-2	4.310	25.692
animal 3	er-3	4.620	27.540

When we plot the individual animal data in Figure 2, the resulting equation with an $R^2 = 1$ demonstrates the presence of biochemical homogeneity. This is reassuring in that we now have an equation that effectively passes through the origin (y intercept = 0.0063) and defines the relationship of structure to function in biology by rule. In effect, we can now predict biological outcomes with the required level of assurance ($R^2 = 1$).

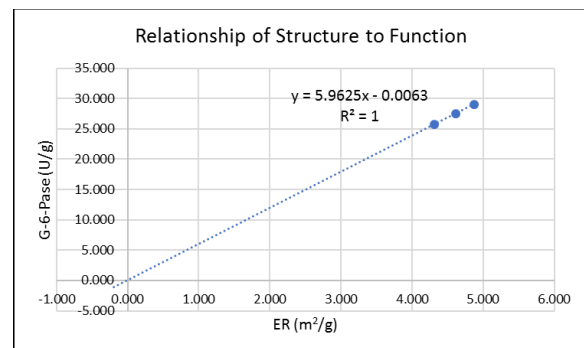


Figure 2 The linear relationship of G-6-Pase activity to the surface area of the er has an $R^2 = 1$. The equation solves for y (units of enzyme activity) when an ER membrane surface area (m²/g) is assigned to x.

If we reverse the axes of the plot in Figure 2, we get an equation that uses enzyme activity to solve for ER surface area (Figure 3).

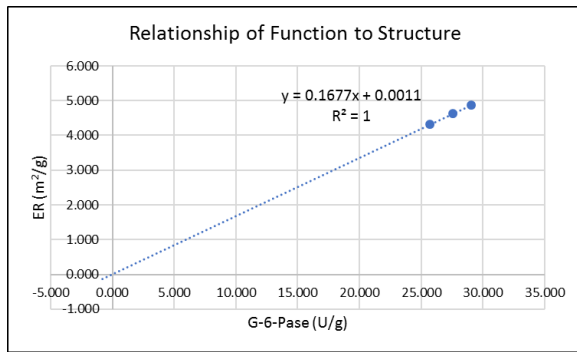


Figure 3 This equation allows us to predict the surface area of the er from the biochemical activity of G-6-Pase.

Next, in an Excel worksheet, we can use the equation of Figure 3 to predict the surface areas of the er membranes from G-6-Pase activities (Figure 4). When applied to G-6-Pase measured in tissue fractions (Table 3): E (extract), N (nuclear), M (heavy mitochondrial), L (light mitochondrial), and P (microsomal) fractions; (note that the supernatant fraction (S) is without membranes), the postulates of deDuve behave as expected a second time.

g6p(U/g)	enter Y→	22.620
	slope	y intercept
	0.1677	0.0011
er(m ² /g)	X=	3.794

Figure 4 A simple calculator - programed in an Excel worksheet - is shown predicting an er surface area (3.794 m²/g) from an enzyme activity (22.62 U/g). Recall that in a linear equation ($y = mx + b$), m is the slope and b the y intercept. When the y intercept approaches zero (e.g., 0.0011), it effectively passes through the origin.

Table 3 The surface areas of er membranes (green overlay) in tissue fractions were predicted using the equation shown in Figures 3 and 4. Recoveries were calculated for F/T, H/T, and F/T, where F=fractions (en+m+l+p+or-s), T=intact tissue, and H=homogenate. Paper 1 (original) and predicted recoveries are listed.

S(er) Predicted from G-6-Pase Activity							
F	F		F/H	F/H	T	H/T	F/T
	s(er)	g-6-pase	g-6-pase	s(er)	s(er)	s(er)	
e	3.794	22.620			4.870		
n	0.715	4.256	26.876 ←H→	4.509	4.310	4.509	
m	0.611	3.639			4.620		
l	0.409	2.435			13.800		
p	2.473	14.740			4.600	4.600	4.600
s	0.072	0.420	25.490 ←F→	4.280			4.280
paper 1	recoveries		94.66%		94.60%		84.30% 80.50%
predicted	recoveries		94.84%		94.92%		98.03% 93.05%

Figure 5 plots the morphological recoveries given in Table 3. Although the F/H recoveries are comparable for both approaches, the predicted recoveries show a clear improvement with membrane recoveries closer to 100%.

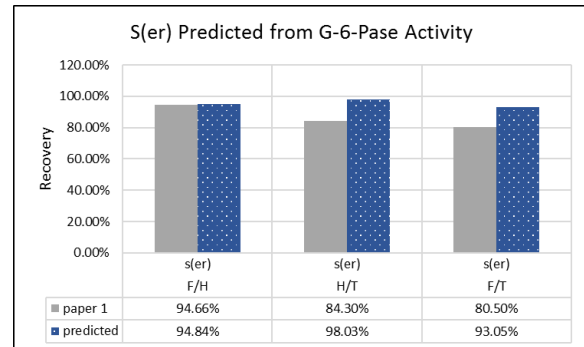


Figure 5 A recovery equal to 100% represents the best possible outcome, wherein nothing is lost or gained because of the fractionation. The figure illustrates the ability of the $R^2 = 1$ equation to predict the amount of ER membranes in the homogenate (H) and fractions (F); T identifies the amount of hepatocytic ER membrane estimated in the intact tissue.

Notice in the plot above that predictions derived from the biochemical homogeneity equation ($R^2 = 1$ equation) were more successful at detecting morphological membranes in tissue fractions than those based on the original stereological methods of Paper 1. More importantly, perhaps, the calculator shown in Figure 4 generated the results in just a few minutes.

Since Paper 1 also included data for several other membrane-bound marker enzymes, they too were examined for homogeneity by subjecting them to $R^2 = 1$ test. The good news is that they all passed: cytochrome oxidase (CYOX) for the inner mitochondrial membrane (IMIM), monoamine oxidase (MAO) for the outer mitochondrial membrane (OMIM), and 5' nucleotidase for the plasma membrane (PM). Since the complete set of calculations are included in the worksheets, only one plot per enzyme is given here.

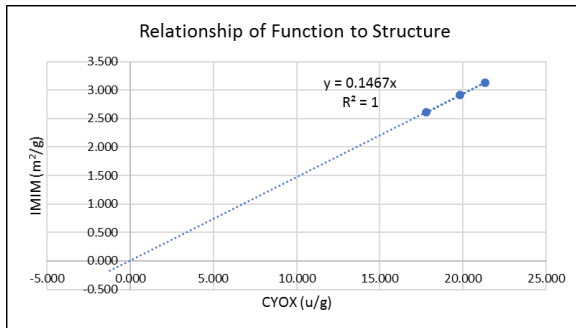


Figure 6 The equation predicts the surface area of the inner mitochondrial membrane (IMIM) - with an $R^2 = 1$ - from cytochrome oxidase (CYOX) assayed in homogenates (E+N).

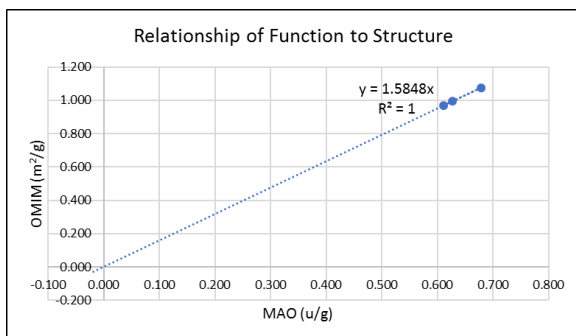


Figure 7 The equation predicts the surface area of the outer mitochondrial membrane (OMIM) - with an $R^2 = 1$ - from monoamine oxidase (MAO) assayed in homogenates (E+N).

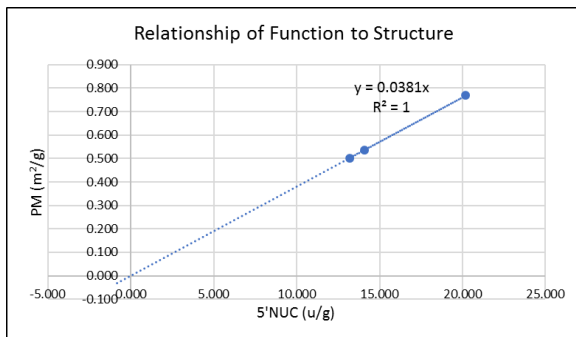


Figure 8 The equation predicts the surface area of the plasma membrane (PM) - with an $R^2 = 1$ - from 5'nucleotidase (5'NUC) assayed in homogenates (E+N).

Summary: (Paper 1)

- Data analyzed at the level of individual animals can be fitted to linear curves (Equations 1 and 2) that display $R^2 = 1$.
- The existence of $R^2 = 1$ curves supports the postulates of deDuve by demonstrating

mathematically a direct relationship between structure and function.

- The postulates gain further support from the $R^2 = 1$ curves by their ability to predict surfaces areas in tissue fractions with recoveries at or near 100%.

Paper 2 (original data): The objective of this paper (Losa et al., 1978) was to identify membranes in the tissue fractions of biochemistry by quantifying intramembrane particles seen in freeze-fracture replicas. In the microsomal fraction, for example, 63% of the membranes were identified as ER with freeze-fracture and 62% with G-6-pase cytochemistry. The remaining membranes included PM + IMIM (20%) and OMIM (17%). Earlier, however, Beaufay et al., 1974 reported that the percentage of the ER in the microsomal fraction was closer to 77%.

Paper 2 (reworked data): Using $R^2 = 1$ equations, we can predict the membrane composition of the microsomal fraction from its marker enzyme data. First, however, we need to show that the equations developed with one set of animals continue to hold true when applied to a new set of animals displaying different body and liver weights. This will tell us whether the rules detected with one group of animals apply to other groups sharing the same species and liver related genes. In other words, does genetic homogeneity translate into phenotypic homogeneity?

To see if the $R^2 = 1$ equations generalize, we can compare the predictions coming from the two different sets of animals used in Papers 1 and 2. The top panel of Figure 9 shows remarkably similar distributions for ER membrane surface areas (S) and G-6-pase activities (U) in the membrane containing fractions (N, M, L, P) for Papers 1 and 2. When – for each paper - the individual surface areas are plotted against their

respective enzyme activities, the relationship of structure to function is defined by exactly the same $R^2 = 1$ equation (bottom panel). In effect, the data of both papers 1 and 2 adhere assiduously to the postulates of deDuve.

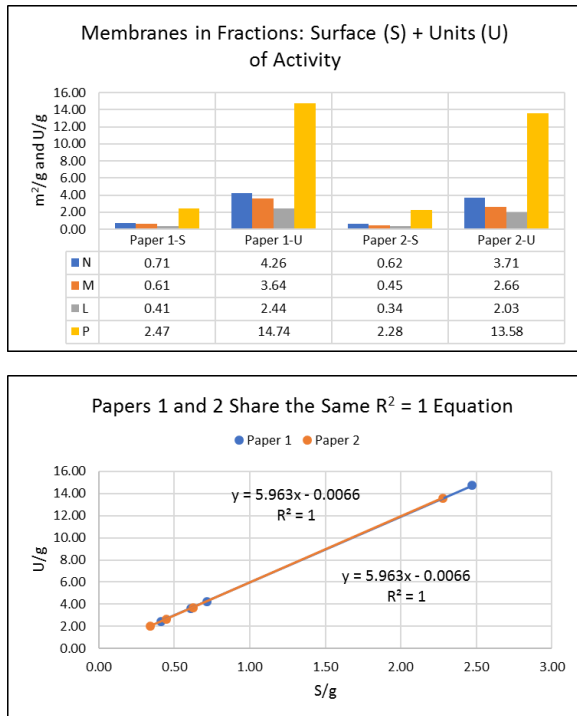


Figure 9 The plots illustrate that the same mathematical relationship exists between the data of Papers 1 and 2 (ER surface vs. activity of its marker enzyme G-6-Pase).

Now we can turn our attention to the freeze fracture and cytochemical data of Paper 2. When we use the $R^2 = 1$ equations of Paper 1 to predict membrane surface areas [plasma membrane (PM), inner mitochondrial membrane (IMIM), endoplasmic reticulum (ER), and outer mitochondrial membrane (OMIM)], from the biochemical data of paper 2, we can plot the new estimates next to the original ones from freeze-fracture (Figure 10). The figure indicates that the two estimates fail to agree.

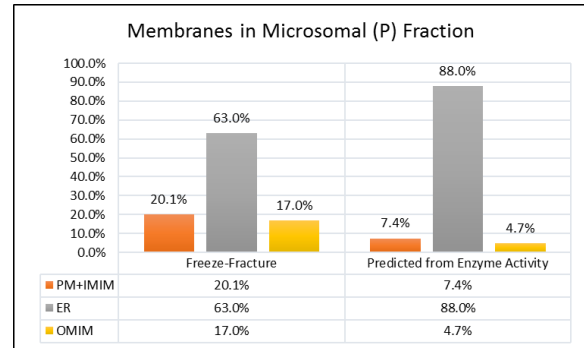


Figure 10 The distribution pattern of cellular membranes in the microsomal (P) fraction estimated with freeze-fracture differs from those predicted from enzyme activities.

How might we explain these differences?

1. The intramembrane particle densities, which were used to identify microsomal membranes, showed considerable overlap for the PF faces in the intact tissue standards and the PF face of the PM and IMIM in fractions, as suggested in Figure 4 and Table I; Paper 2). Distinguishing RER from the OMIM might have been the most problematic (Figure 4, Paper 2). These factors may have contributed to the higher than expected values for the PM+IMIM and OMIM values shown in Figure 10.
2. As reported by Blouin et al. (1977), 30% of the plasma membranes in the liver derive from nonhepatocytic cells. Since the contaminating plasma membranes are not known to carry the marker enzyme 5' nucleotidase, they would be invisible to the predicted value based on enzyme activity, but possibly visible to freeze-fracture. This might help to explain the higher values for the combined PM+IMIM membranes in the P fraction (Figure 10).

In the discussion of Paper 2, Losa et al., (1977) estimated the amount of ER membrane in the P fraction – assuming biochemical homogeneity – and arrived at a value somewhere between 76-78%. [Note: If we divide the corrected surface areas of the membranes in the intact tissue (Paper 1) by the sum of the enzyme activities in

the four fractions – N+M+L+P (Paper 2), we get a rough estimate for the membrane surface area associated with a unit of enzyme activity (S/U).] By multiplying the S/U values by their respective enzyme activities in the P fraction (Paper 2), we can estimate the membrane surfaces (Figure 11). Notice that this new value for the ER (80.11%) comes closer to the 76-78% suggested by Losa et al. (1977) and the 77% value of Beaufay et al. (1974).

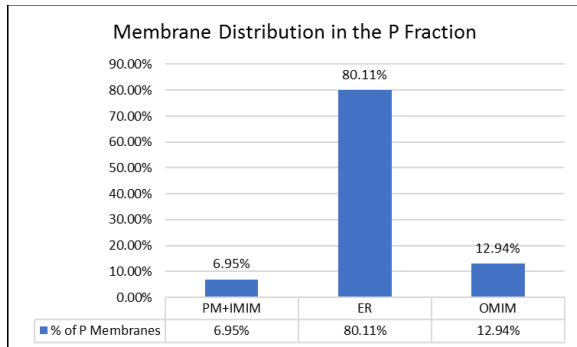


Figure 11 This distribution of membranes in the P fraction of Paper 2 is based on a rough estimate based on data coming from two different sets of animals (Papers 1 & 2) without the benefit of the $R^2 = 1$ equations.

Summary: (Paper 2)

- When – for Papers 1 and 2 - G-6-Pase activities are plotted against their predicted ER surface areas, both data sets generated the same equation with an $R^2 = 1$. Such a finding offers further evidence in support of deDuve's postulates.
- The distribution of different membrane types in the P fraction of rat livers can be estimated using freeze-fracture, cytochemistry, and $R^2 = 1$ equations. However, each estimate produced a somewhat different result.

Paper 3 (original data): The objective of the study was to consider the relationship of ER membrane surface areas to their constitutive marker enzyme activities in homogenates and tissue fractions (Bolender et al., 1980). When relative amounts of ER marker enzyme activities

were compared to the surface areas of their membrane locations, variable distributions were found for G-6-pase and NADPH cytochrome c reductase (NADPH-CCR), but not for esterase. G-6-Pase cytochemistry was used to identify ER membranes in fractions, but the recoveries indicated that roughly 30% of the membranes were not being detected (F/H = 95.8%, H/T = 74.06%, and F/T = 70.7%. (Recall that in Paper 1, the H/T and F/T recoveries predicted 98% and 93%.)

In summary, the results of Paper 3 offered evidence both for and against the postulate of biochemical homogeneity.

Paper 3 (reworked data): In revisiting these results, we will use the $R^2 = 1$ equation for G-6-Pase from Paper 1 to predict the ER surface areas in the homogenate and fractions from the enzyme activity data reported in Paper 3. In turn, we will use these ER surface areas (based on G-6-Pase) to interpret two other ER marker enzymes - esterase and NADPH-CCR.

When the $R^2 = 1$ equation for G-6-Pase of Paper 1 is applied to the biochemical data of the fractions reported in Paper 3, we continue to generate an equation with an $R^2 = 1$ (Figure 12). Once again, two different sets of animals having different body and liver weights share the same relationship of structure to function - more evidence in support of deDuve's postulates.

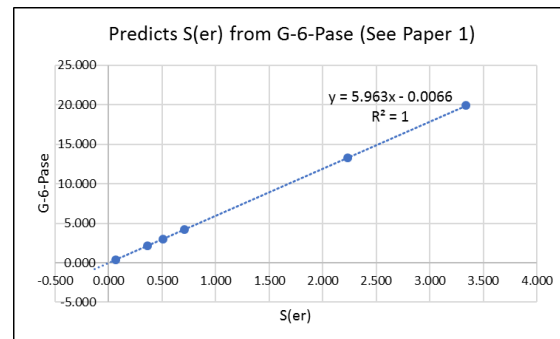


Figure 12 When the equation of Paper 1 is used to predict ER surface areas from the biochemical data of tissue fractions in Paper 3, the result is a curve with an $R^2 = 1$. Recall that deDuve's postulates assume such a result.

Does this $R^2 = 1$ approach ever fail? Yes. If we take the ER surfaces generated above with the $R^2 = 1$ equation of Figure 12 and plot them against the activities of esterase and NADPH-CCR, notice what happens. We no longer get an $R^2 = 1$ outcome. Several data points have left the regression lines.

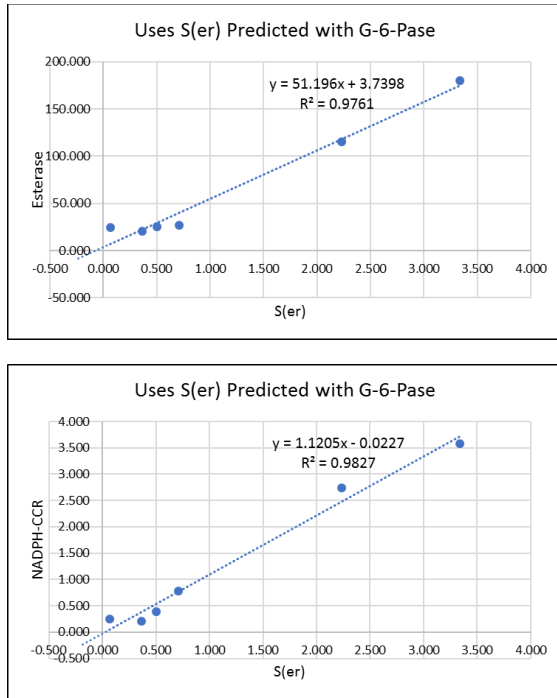


Figure 13 When the distribution of ER membrane surface areas is based on G-6-Pase activity and used as a basis for plotting other ER marker enzymes (esterase, NADPH-CCR), several points no longer fall on the line and the R^2 falls to 0.9827. Notice that the patterns of the points and the y intercepts of the two curves are different.

Why did we have success in Paper 3 with G-6-Pase, but not with esterase and NADPH-CCR? One explanation to consider is the possibility that the ER appears homogeneous, but in fact, it consists of two, slightly different homogeneities – one for the SER and another for the RER. Were this the case, then we would expect to see the same distribution pattern for both the esterase and NADPH-CCR points in Figure 13, being tied as they both are to the same G-6-Pase prediction of membrane surfaces. Clearly, this was not the case. Biases and mistakes aside, a remaining possibility may

offer a plausible explanation. To wit, all three enzymes (G-6-Pase, esterase, and NADPH-CCR) may have homogeneous ERs, but slightly heterogeneous SERs and RERs.

Since $R^2 = 1$ equations are good at finding homogeneities, but not heterogeneities, we need equations better suited to the task of detecting heterogeneities. If we write pairs of linear equations in two unknowns and solve them simultaneously, we can determine the enzyme densities (ED = units of activity/membrane surface) of the SER and RER membranes (Bolender, 1981). This calculation should tell us if these ER membrane subcompartments are the same or different.

Since we know the surface area of the SER and RER in the intact tissue and the total G-6-Pase activity in the homogenate for three animals (Paper 1), we can write three linear equations consistent with the homogeneity postulate. This gives us three pairs of simultaneous equations (animals: 1-2, 1-3, and 2-3) that Mathematica (Wolfram Research, Inc.) can solve for us. A successful solution gives pairs of enzyme densities (ED) - one for SER and another for RER.

The linear equations in two unknowns [ED(ser); ED(rer)] take the following form:

Animal 1

$$S(ser) * ED(ser) + S(rer) * ED(rer) = U/g \quad (4)$$

Animal 2

$$S(ser) * ED(ser) + S(rer) * ED(rer) = U/g \quad (5)$$

Animal 3

$$S(ser) * ED(ser) + S(rer) * ED(rer) = U/g \quad (6)$$

where:

$$ED(ser) = (U/g)/(S(ser)/g)$$

$$ED(rer) = (U/g)/(S(rer)/g) .$$

The equations and solutions appear below.

animal 1: $S(\text{ser}) \cdot \text{ED}(\text{ser}) + S(\text{rer}) \cdot \text{ED}(\text{rer}) = U(\text{G-6-Pase})$
 animal 2: $S(\text{ser}) \cdot \text{ED}(\text{ser}) + S(\text{rer}) \cdot \text{ED}(\text{rer}) = U(\text{G-6-Pase})$
 animal 3: $S(\text{ser}) \cdot \text{ED}(\text{ser}) + S(\text{rer}) \cdot \text{ED}(\text{rer}) = U(\text{G-6-Pase})$

Mathematica requires the following format, wherein x represents the enzyme density for the SER and y for that of the RER:

Solve[{1.90 x + 2.97 y == 27.421, 1.44 x + 2.88 y == 24.267}, {x, y}]
 Solve[{1.90 x + 2.97 y == 27.421, 1.96 x + 2.66 y == 26.103}, {x, y}]
 Solve[{1.44 x + 2.88 y == 24.267, 1.96 x + 2.66 y == 26.103}, {x, y}]

{{x -> 5.77267, y -> 5.53971}}
 {{x -> 5.97765, y -> 5.40858}}
 {{x -> 5.85671, y -> 5.49769}}

Notice that the values (EDs) for X (ser) are slightly larger than those for Y (rer). In effect, the SER and RER are heterogeneous with respect to one another.

If we substitute the values for X and Y back into the equations, we can compare the predicted values for G-6-Pase to the ones originally measured (Figure 14). Notice that the two values are almost identical.

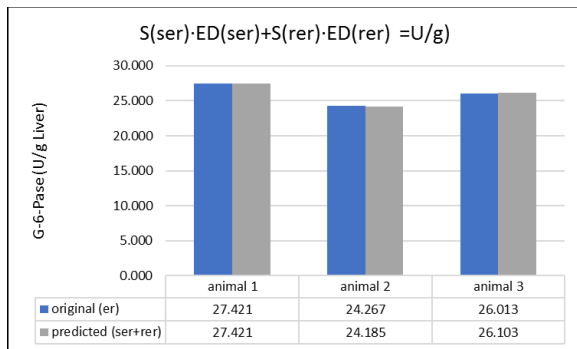


Figure 14 The units of G-6-Pase activity estimated for the SER and RER in three animals matches the activity of the ER assayed in the same animals biochemically.

Since the EDs of the SER and RER appear to differ by such a small amount, is the difference significant? If we run a double tailed t test on the data and plot the results, the answer is yes (Figure 15). Not only does a difference exist, it is highly significant (P = 0.0056).

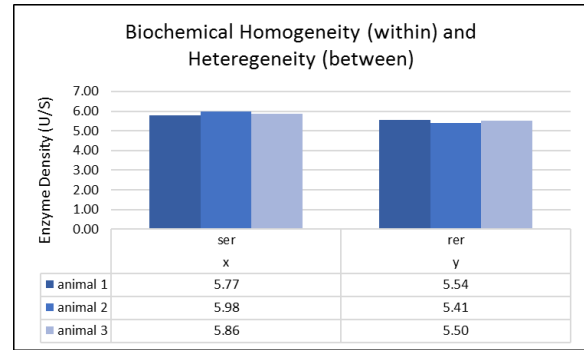


Figure 15 The enzyme density of the SER is greater than that of the RER by 7% (P=0.0056). In effect, the homogeneity of the ER reflects two underlying heterogeneities.

Notice the ability of enzyme densities (ED) to define mathematically a fundamental concept of biology – the relationship of structure to function. They become predictive when plotted as a linear equation ($R^2 = 1$), can quantify the concentration of a given marker enzyme when it exists at different morphological locations, and even unfolds the complexity of a biological change (Bolender, 1981).

Finally, we need to address the key finding of biochemical heterogeneity in Figure 5 of Paper 3, which used G-6-Pase cytochemistry to identify membranes of the ER in tissue fractions. If we recalculate the relative specific activities (RSA) for G-6-Pase using the enzyme activities of the fractions and the ER surfaces predicted from these activities with the $R^2 = 1$ equation of Paper 1, we find evidence for homogeneity, not heterogeneity – at the ER level. In effect, the data of Paper 3 now support deDuve's postulates of biochemical homogeneity and single location.

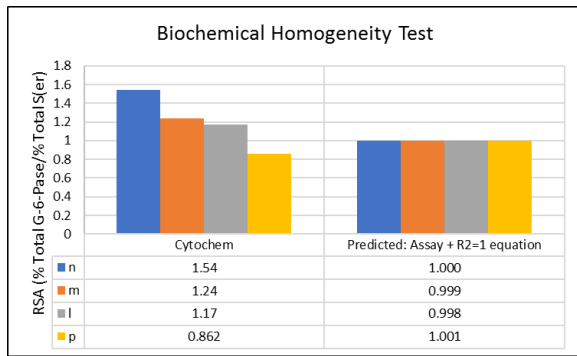


Figure 16 The relationship of marker enzyme activity to ER membrane surface area depends on how the ER membranes are identified in the four fractions (N, M, L, P). Cytochemistry detects biochemical heterogeneity, whereas $R^2 = 1$ equations find biochemical homogeneity.

Before leaving Paper 3, we need to tidy up a few loose ends. Recall that when using the ER surface areas predicted from G-6-Pase activity, the expected $R^2 = 1$ equations failed to materialize for esterase and NADPH-CCR (Figure 13). If, however, we use the standard method for generating these equations (Equation 1, Table 2, Figure 2), the $R^2 = 1$ equations appear, along with recoveries close to 100%. The recalculated equations are given in Figure 17.

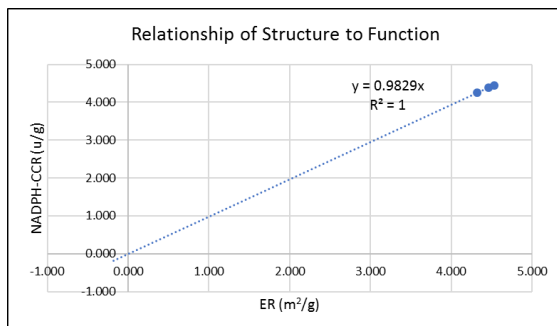
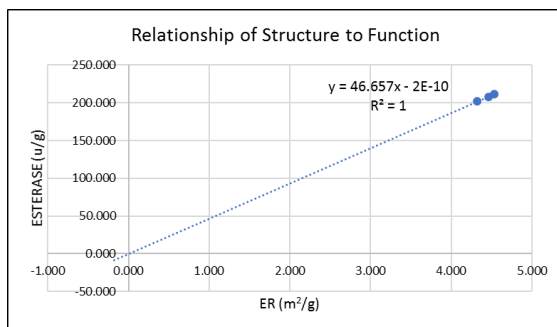


Figure 17 When related to the surface area of the ER, both esterase and NADPH-CCR display $R^2 = 1$ equations.

Since the intact tissue values for the ER but not SER and RER were included in Paper 3, enzyme densities for these locations could not be calculated, using equations 4, 5, and 6.

Summary: (Paper 3)

- The $R^2 = 1$ equation for G-6-Pase from Paper 1 predicted the surface areas of the ER in the fractions of Paper 3 (using data from three different animals) with an $R^2 = 1$. Such a result supports the postulates of biochemical homogeneity and single location.
- When the predicted er surface areas in the fractions were plotted against their corresponding enzyme activities for esterase and NADPH cytochrome c reductase, the resulting equations did not display R^2 s = 1. This suggested that the subcompartments of the ER – the SER and RER – were heterogeneous (they had different EDs).
- The SER and RER subcompartments of the ER were tested for homogeneity by solving three sets of simultaneous equations. The results indicated that the SER membranes had a 7% higher concentration of G-6-Pase per unit of membrane surface area than those of the RER.
- It appears likely that ER marker enzymes, such as G-6-Pase, esterase, and NADPH-CCR, are distributed unequally across the membranes of the SER and RER. This may be due to the presence of ribosomal attachment sites on the RER consuming territory that would otherwise belong to the marker enzymes. This could explain the lower enzyme concentrations on the RER.

Predicting Biochemistry from Biochemistry

With evidence in support of the postulates of biochemical homogeneity and single location, we can now turn our attention to the problem of assembling predictive networks for biochemical data – across publications. We begin the process by identifying quantitative patterns in biochemical data, using mathematical markers and connection ratios.

Identifying biochemical patterns: Amar-Costesec et al., (1974) published an extensive collection of biochemical assays from the rat liver, including data from tissue homogenates (E+N) and fractions (N, M, L, P, S). The data set included assays for 22 different enzymes, coming from hundreds of experiments.

We can use this data set to look for patterns of similarity. By generating triplets (22 enzyme activities taken three at a time), and relating them to the ratios of their activities, we can see the extent to which biology orders its enzyme activities in rat liver hepatocytes (Figure 18). The plot (top panel) suggests that the proportions of one enzyme activity to another is being highly orchestrated by biology. Each rosette represents a unit of common connectivity. The enlarged portion of the plot (bottom panel) shows that the same pattern – the ratio of three different enzyme activities (triplets) - occurs many times with many different groupings of enzymes.

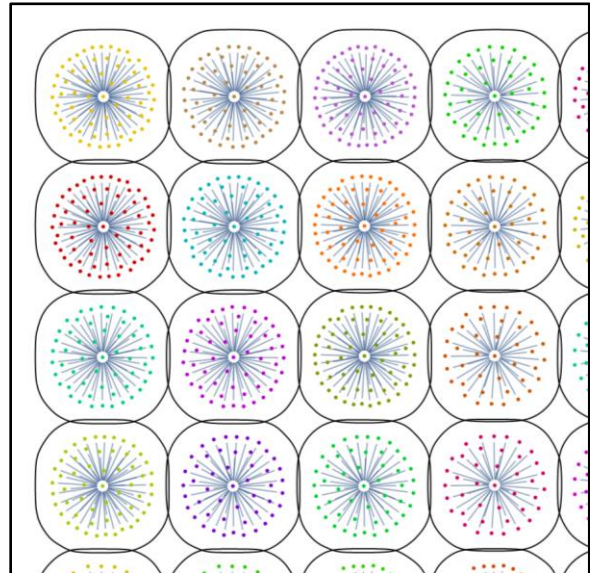
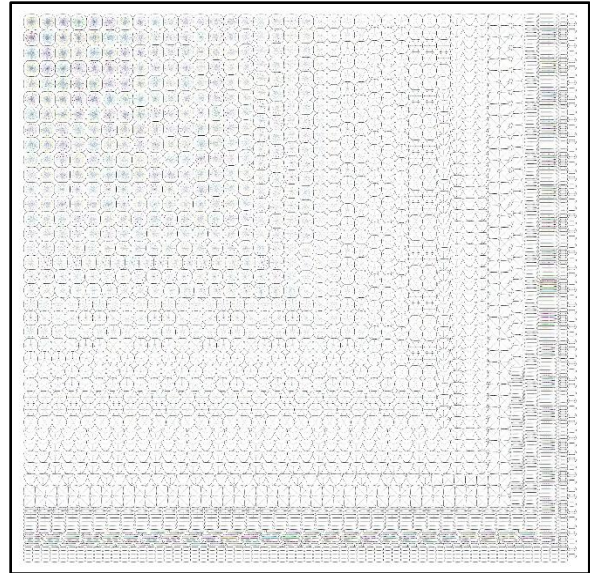


Figure 18 Top panel: The plot illustrates the connectivity of 22 enzymes in the rat liver. Bottom panel: The enlargement shows that many different combinations of enzyme activities frequently share the same proportions. The central dot identifies a connection ratio, whereas the surrounding dots represent mathematical markers (enzyme triplets) sharing that ratio. (Plots derived from data published by Amar-Costesec et al., 1974.)

If we consider just G-6-Pase and its relationship to the remaining 21 enzymes, we can see how one enzyme fits into the larger picture of biological complexity (Figure 19). These repeated patterns - an expression of stoichiometry – identify the downstream

expressions of genetic activity. Although these patterns signal the presence of underlying biological rules, how does biology know when and where to apply them? Where do these rules come from? Are they coded somewhere?

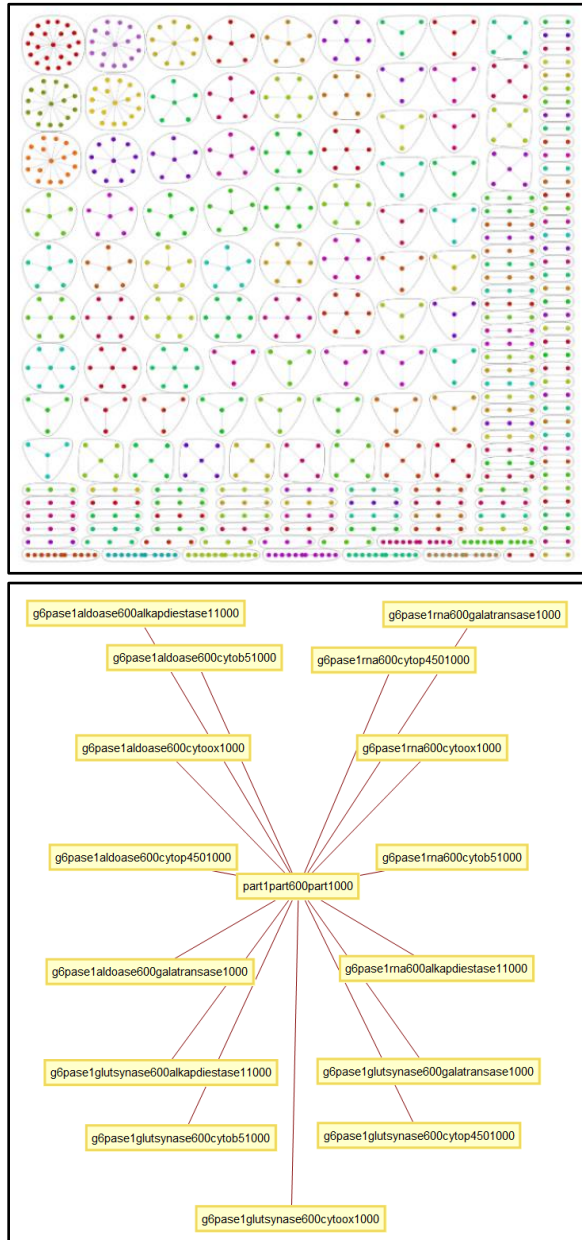


Figure 19 Top panel: The plot shows the relationship of G-6-Pase to the remaining 21 enzyme activities (original data from Amar-Costesec et al., 1974). Bottom panel: The rosette in the upper left corner of the top panel is shown with the mathematical markers (periphery) and connection ratio (center) replacing the points. Enlarge as needed.

Predicting enzyme activities: If, as seen in Figures 18 and 19, the enzymes in liver hepatocytes are related to one another as a ratio of their activities, then the activity one enzyme could be expected to predict the activities of other enzymes. To assemble such a network, as illustrated in Table 4, we can once again use the published data set of Amar-Costesec et al., (1974) and choose G-6-Pase as our reference enzyme (the denominator of the prediction ratios). In turn, we can test the effectiveness of such a network by using it to predict the biochemical results of Papers 1, 2, and 3 from the activity of a single enzyme activity (G-6-Pase = 27.42) entered into Table 4 – the highlighted value.

Table 4 When expressed as ratios of G-6-Pase activity, the resulting network of enzyme data becomes predictive. Note that the table uses the published data of Amar-Costesec et al., Table II; (1974). A value entered for G-6-Pase will predict values for itself and for the remaining enzymes listed in the table. The test (observe vs. predict) was applied to enzyme data of Papers 1, 2, and 3, as shown in the following figures. To run a test, enter a value for G-6-Pase (e.g., 27.42) into the data entry field (highlighted) and press Enter. The results are plotted in Figure 20.

Enzyme	Location	G6Pase=1	27.42	Observe	Predict
5'-nucleotidase	pm	0.559	15.34	15.83	15.34
acid phosphatase	lysosome	0.281	7.70		
aldolase	cytoplasmic	0.394	10.81		
alkaline phosphatase	pm	0.121	3.33		
alkaline phosphodiesterase 1	pm	0.866	23.75		
aminopyrine demethylase	er	0.004	0.11		
b-glucuronidase	lysosome	0.058	1.59		
catalase	peroxisome	2.356	64.61		
cytochrome b5	er	0.950	26.06		
cytochrome oxidase	imim	0.936	25.66	19.65	25.66
cytochrome p 450	er	1.074	29.46		
esterase	er	12.723	348.86		
fumarase	mi	4.733	129.77		
galactosyl transferase	golgi	0.001	0.02		
glucose-6-phosphatase	er	1.000	27.42	27.42	27.42
glucuronyltransferase	er	0.118	3.23		
glutamine synthetase	mi	0.426	11.69		
monoamine oxidase	omim	0.025	0.69	0.64	0.69
n-acetyl-b-glucosaminidase	lysosome	0.341	9.34		
nadh cytochrome c reductase	imim	4.950	135.74		
nadh cytochrome c reductase	er	0.197	5.40		
nucleoside diphosphatase	golgi	4.950	135.74		

For a prediction to be successful, it should generate an equation – comparing observed to predicted values – with an $R^2 \approx 1$. Once again, the curve should pass through the origin – or nearly so. As shown in Figures 20 and 21, most,

but not all the enzymes in play met these conditions.

Paper 1

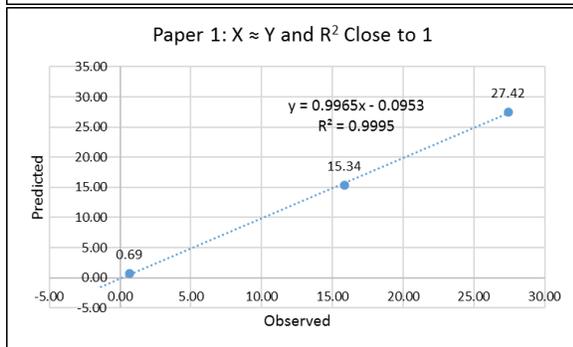
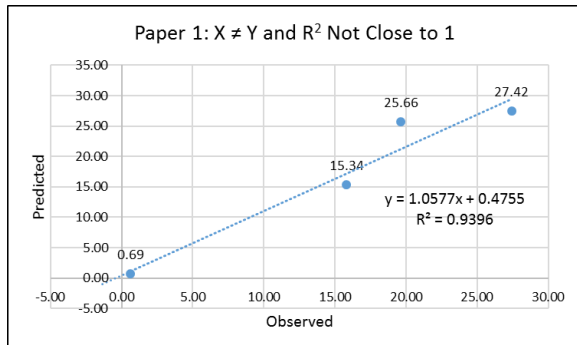


Figure 20 The biochemical data observed and predicted in Table 4 are plotted with four (top) and three enzyme activities. When the cytochrome oxidase point (25.66) is excluded, the equation displays a R^2 close to one (0.9995).

Paper 2

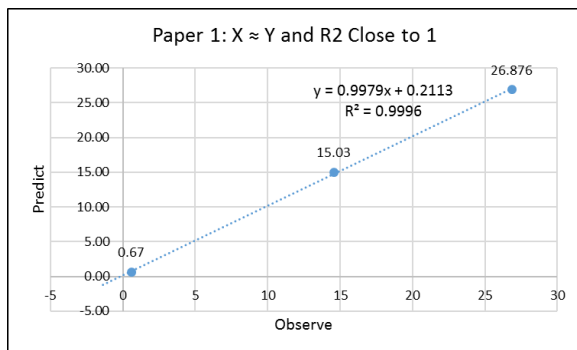


Figure 21 Once again, removing cytochrome oxidase brought the R^2 close to one (0.9996).

Paper 3

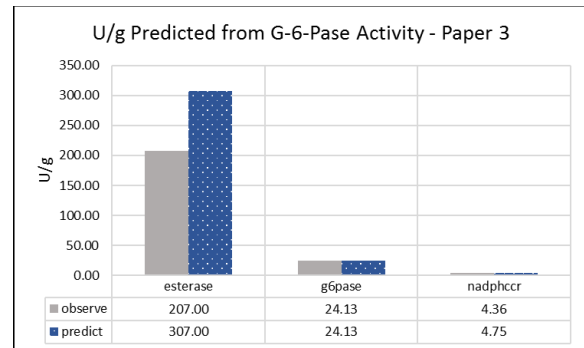


Figure 22 For Paper 3, the biochemical predictions worked for only two of the three marker enzymes. The esterase inconsistency cannot be explained.

Why did some predictions work, but others not? As a practical guideline, predictions for enzyme activities that can be confirmed with $R^2 \approx 1$ equations are the ones most likely to be credible.

The fact that the data of one publication (Amar-Costesec et al., 1974) was successful in predicting the data of several other studies (Papers 1-3) represents a preliminary, but promising outcome. Cytochrome oxidase, however, failed to fit into the expected $R^2 = 1$ pattern it displayed in Papers 1 and 2. Why?

Recall that cytochrome oxidase is attached to the inner mitochondrial membrane, but is derived from both mitochondrial and nuclear DNA (Youfen et al., 2016). By having to serve two sets of rules (mitochondrial and nuclear DNA), it became an outlier. As such, it doesn't belong to an $R^2 = 1$ equation made up of enzymes derived wholly from nuclear DNA (Figures 20 and 21).

Summary (Predicting Biochemistry from Biochemistry):

- The relationship of one enzyme activity to another is defined by a ratio.
- Ratios of enzyme activities display predictive properties with $R^2 \approx 1$.

- Although biochemical networks are largely under the control of nuclear DNA, mitochondrial DNA can also be in play.
- The cytochrome oxidase system – a marker enzyme for the inner mitochondrial membrane - is controlled by both nuclear and mitochondrial DNA.

Predicting Morphology from Morphology

Predicting morphological surface areas: Using the approach just described for biochemistry, we can also predict the amounts of membrane organelles in cells (e.g., hepatocytes). Recall that this is possible because biology defines the relationship of one part to another quantitatively with ratios.

Figure 22 plots two sets of membrane surface areas - animal 1 vs. animal 3 - from Paper 1. Notice that they fit a line with an R^2 close to 1 (0.996) that passes roughly through the origin (0.0116) – properties consistent with biochemical and biological homogeneity.

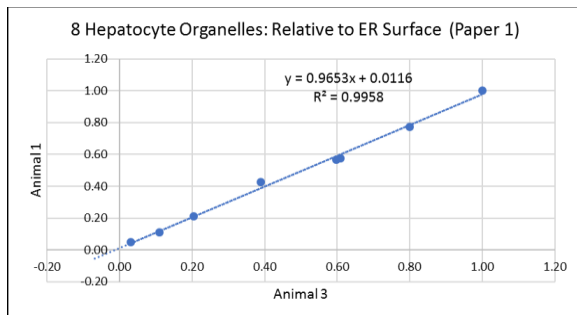


Figure 23 Surface areas of eight organelles are divided by the surface area of the ER for each of two animals. The plot with an $R^2 = 0.9958$ suggests that the two animals contain the same relative amounts of hepatocytic organelles.

In turn, the data of animals 1 and 3 of Paper 1 (Figure 23) were averaged and used to assemble an interactive prediction table (Table

5) – analogous to the one used in Table 4 for biochemistry.

Table 5 When a value for the ER is entered (highlighted field - 4.87), values for the remaining membrane organelles are predicted. When compared to the observed data of a single animal (Paper 1), they show close agreement – as expected (recall Figure 23).

Location	m ² /g	4.87	Observe	Predict	%(O/P)
er	1.000	4.870	4.870	4.870	100%
ser	0.407	1.983	1.900	1.983	96%
rer	0.593	2.887	2.970	2.887	103%
go	0.039	0.192	0.151	0.192	79%
pm	0.109	0.533	0.537	0.533	101%
mim	0.788	3.837	3.900	3.837	102%
omim	0.207	1.007	0.993	1.007	99%
imim	0.581	2.831	2.910	2.831	103%
sum			18.231	18.140	101%

The advantage of such organelle prediction tables is that they derive from the order biology creates in cells with its well-defined ratios. Moreover, such prediction tables, which can be assembled in a few minutes, generate large amounts of new data quickly and cost-effectively. With just an estimate for the ER surface area, for example, we could readily predict surface areas for a panel of other organelles – such as those listed in Table 5. In turn, we can translate the membrane surface areas into enzyme activities.

Consider Paper 3. There were only two estimates reported for the intact tissue (ER and total membranes). If we use Table 5 and enter a value for the ER for each animal, we can predict the missing data (Golgi, plasma membrane, and mitochondrial membranes), as shown in Table 6. In turn, we can check the predictions by calculating recoveries that compare observed to predicted values (sum vs. observed) – e.g., $8.77/9.49 = 92.4\%$.

Table 6 When a value from Paper 3 is entered for the ER, the table predicts surface areas for the Golgi, plasma membrane, and mitochondria. When the sums of the membrane surface areas are compared to the published totals, the recoveries ranged from 92 to 97%. Such results

suggest that the animals in Papers 1 and 3 are reading the same blueprint when populating hepatocytes with organelles.

Location	Animal 2	Animal 3	Animal 4
er	4.53	4.31	4.62
go	0.18	0.17	0.18
pm	0.50	0.47	0.51
mim	3.57	3.40	3.64
sum	8.77	8.35	8.95
observed	9.49	8.95	9.22
recoveries	92.4%	93.3%	97.0%

Summary (Predicting Morphology from Morphology):

- *The surface areas of membrane organelles relate to one another as ratios.*
- *Membrane surface areas can be predicted from ratios of membrane surface areas.*

Biological Homogeneity

If the genetic coding for the liver has remained largely unaltered over time, then the downstream relationships of structure to function should be conserved similarly across animal species. In effect, homogeneity in the genotype would be expected to predict homogeneity in the phenotype.

To test this **postulate of biological homogeneity** in the phenotype, we need to show that the patterns and rules detected in rat liver hepatocytes continue to exist - largely unaltered - in the hepatocytes of other species.

At this point, our job becomes more difficult because the assumptions of experimental uniformity enjoyed in Papers 1 to 3 - animal age and sex, fasting, sampling, and exposure - often no longer apply. Although comparing the data of one species to that of another continues to require a comparable amount of preprocessing (section related corrections and standardization), the data published for humans

and other species tend to be sparse and often incomplete for our purposes here. This means that the generalizing arguments made earlier with $R^2 = 1$ equations will be replaced by those based on the available data and predictions (Note that the calculations are given in the Appendix). We begin by looking for similarities in hepatocytic organelles between humans, rats, and dogs in four papers.

Koch, M. M. et al., 1978, A stereological and biochemical study of the human liver in uncomplicated cholelithiasis: The main point of the first example is to show that we can start with a single data point – biochemical or morphological - and end up with largely the same results. Such an outcome would be expected when the same rules are in play.

Using human biopsy specimens, Koch et al., (1978) reported membrane data related to the cytoplasm of hepatocytes. These data were converted to a gram of liver (on the assumption that the hepatocytic cytoplasm represents 71% of the liver volume and that the human liver has a density of 1.07 g/cm^3) and corrected for section related artifacts (see Table III of Paper 1). The results (human data for organelle surface areas per gram liver) were plotted against comparable data from the rat, which were predicted from the human value for the ER using the equations of Paper 1 (Figure 24). Notice that the results were roughly similar between the two species for the ER, plasma membrane (PM), and outer mitochondrial membrane (OMIM), but not for the inner mitochondrial membrane (IMIM) – the perennial outlier.

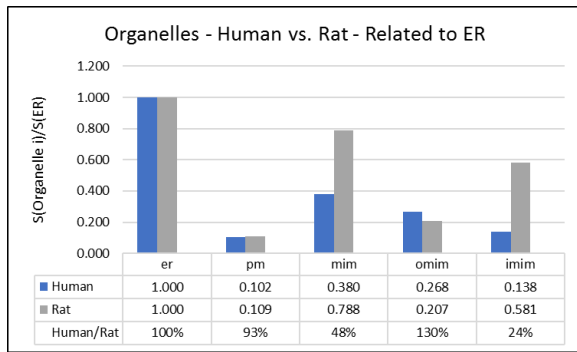


Figure 24 Surface areas of organelles in human hepatocytes are compared to those in the rat, which were predicted from the human biopsy estimate for the ER surface area using the data of Paper 1. The results - expressed relative to the surface area of the ER in each species - show similar patterns - except for the inner mitochondrial membrane. (Data adapted from Koch et al., 1978 and Paper 1)

Next, we can use the one enzyme activity reported in the Koch paper (NADPH-CCR) to generate a second set of estimates, using the biochemical data coming from the rat liver. Since the assay for NADPH-CCR came from a microsomal (P) fraction, it was scaled up to the homogenate on the assumption that the P fraction contained 63% of the total activity (see Table III of Paper 3). Next, a prediction table like the one shown in Table 4 was assembled for NADPH-CCR (now expressed as a homogenate) by dividing all the enzyme activities by that of NADPH-CCR. This generated a list of marker enzyme activities for the human liver (using the data of Amar-Costesec et al., 1974; Table II) adjusted to the expected proportions. In turn, these predicted marker enzyme activities were used to predict their corresponding membrane surface areas - in the intact tissue - using the $R^2 = 1$ equations of Paper 1. In short, a single data point - a microsomal estimate for NADPH-CCR - was used to predict membrane surface areas (homogenate) for the plasma membrane (5'Nucleotidase), outer mitochondrial membrane (MAO), and inner mitochondrial membrane (Cy0x); see Table 8. The results, which appear in Figure 25, are once again expressed relative to the ER surface area. They

suggest that the $R^2 = 1$ equations from the rat did a much better job at predicting the ER, PM, and OMIM in humans than for the IMIM.

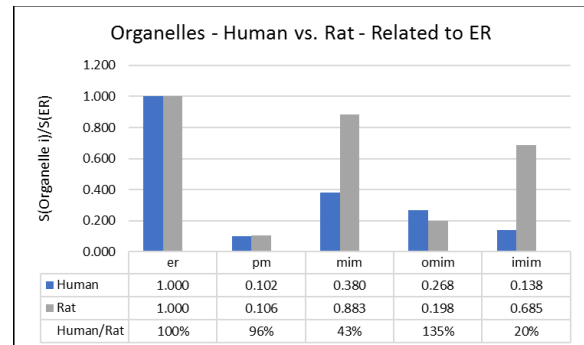


Figure 25 The second prediction - based on the biopsy estimate for NADPH-CCR - resembles the first (Figure 24). (Data adapted from Koch et al., 1978, Amar-Costec et al., 1974 - predicted marker enzyme activities, and Paper 1 - predicted membrane surface areas from predicted enzyme activities.)

By including membrane surface areas and a single enzyme activity (NADPH-CCR), the Koch paper offered several options for reworking the data within the framework of biological homogeneity. The patterns displayed by Figures 24 and 25 show that predictions based on either morphology or biochemistry can produce surprisingly similar outcomes - even when they relied on data coming from two (Figure 24) or three (Figure 25) different papers. This suggests that the biology literature contains research data quite capable of playing by the same rules. The large discrepancy seen for the surface area of the inner mitochondrial membrane is consistent with the results seen earlier for this outlier (Figures 20, 21).

Roessner, A. et al., 1978, Ultrastructural Morphometric Investigations on Normal Human Liver Biopsies: In this paper, we consider a second set of membrane data coming from the human liver. Biopsies from 14 normal adults (male and female) were used to estimate the surface areas of hepatocytic organelles. The raw estimates were corrected for section related biases (see Paper 1),

converted to a gram of tissue, and, in turn, expressed as proportions [S(Organelle_i/S(ER))] (Figure 26-top), and then as concentrations (m²/g liver) (Figure 26-bottom).

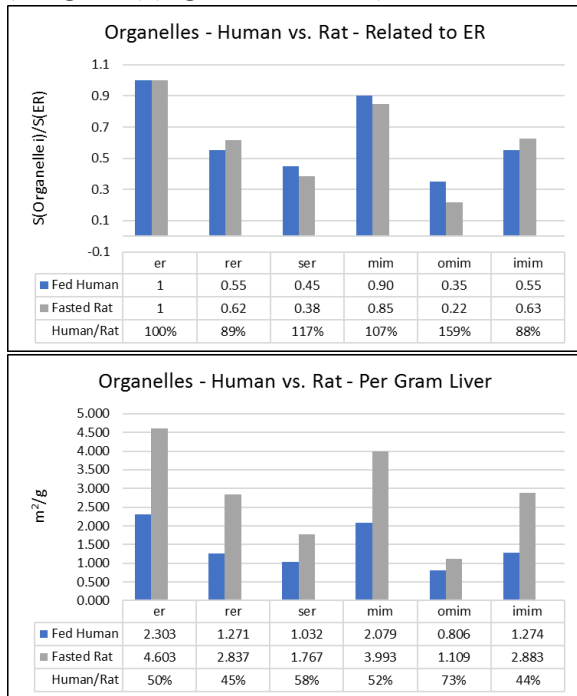


Figure 26 When expressed as ratios relative to the ER, the patterns of hepatocytic organelles in humans and rats display remarkably similar patterns (top). However, when expressed per gram of liver, the fed humans display only about half the membranes seen in fasted rats (bottom). (Data adapted from Roessner et al., 1978 and Paper 1)

Figure 26 indicates that organelles in human and rat hepatocytes occur in roughly the same proportions relative to the ER (top), but, when related to a gram of liver, the fasted rat contains roughly twice the amount of each organelle. Why? Given the homogeneity postulate, we could readily attribute similar ratios to similar DNA, but the m²/g data offer more of a challenge. Notice that the rats were fasted, but the humans not. Glycogen stores, which account for about 20% of the cytoplasmic volume in hepatocytes, disappear in fasted rats. This means that a fasted gram of liver would have had to increase by 20% the number of hepatocytes contained therein to weigh one gram. However, this still leaves 80% of the

difference unexplained. Now let's try a basic metabolic rate (BMR) argument. The BMR (cal/kg/day) of rats is about 96 and that of humans 25 (Holliday, 1967) – a difference of roughly 4 to 1. This suggests that the rat with its higher metabolic rate would require a liver capable of delivering more energy – per gram. Consequently, we would expect the hepatocyte to contain more of everything, including ER, mitochondria, et cetera – all in keeping with its expected ratios (see, for example, Table 5). In effect, the BMR argument could readily account for the elevated organelles shown in Figure 26 (bottom).

A lesson to take from Figure 26 is one of perception. The same data set can be interpreted as a consistency (top) or as an inconsistency (bottom). Note that ratios detect rules, whereas absolute values and concentrations (e.g., m²/g) appear to be detecting rules adapted to a given species (human vs. rat) or to a local set of conditions (fed vs. fasted).

In summary, Figure 26 (top) suggests that both humans and rats share a common blueprint, but that the blueprint comes with an ability to scale (Figure 26 (bottom)). Both findings, however, are consistent with the postulate of biological homogeneity.

de-la-Iglesia, F. A. et al., 1976, Quantitative microscopic evaluation of morphometry of the endoplasmic reticulum in developing human liver: Biopsies taken from the livers of male and female volunteers – ranging in age from 10 to 18 years – are compared to values coming from adult male rats (Paper 1) in figure 27. One group was fed, the other not. Although the pattern for the ER and Golgi were similar in both species, it was different for the SER and RER.

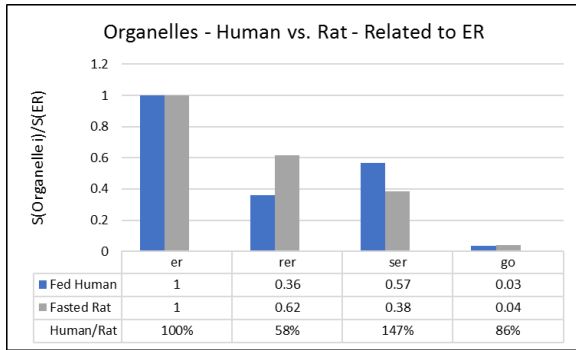


Figure 27 With corrections applied, the surface areas of the ER and Golgi displayed similar distributions, whereas those of the RER and SER did not. (Data adapted from de-la-Iglesia et al., 1976 and Paper 1)

Hess, F. et al., 1973, Morphometry of the Dog

Liver: Normal Base-Line Data: In Figure 28, biopsies obtained from 4 adult female dogs (fed) were compared to the adult male rats (fasted) of Paper 1. The comparison suggests a similar pattern for the ER membranes, but once again not for those of mitochondria.

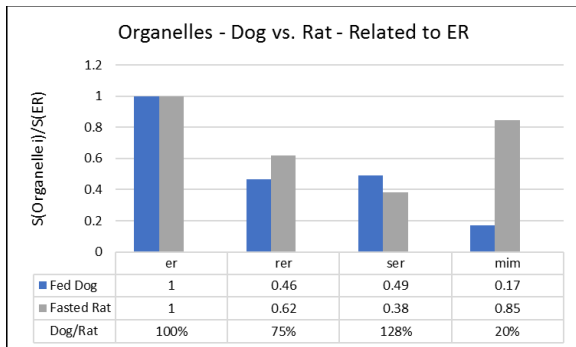


Figure 28 When corrected and expressed relative to the surface area of the ER, the ER of both species appear similar, but not the membranes of mitochondria. (Data adapted from Hess et al., 1973 and Paper 1)

Summary: (Biological Homogeneity)

- $R^2 = 1$ equations and predictive ratios (biochemical and morphological) can be similar within and across animal species.
- The absolute and relative amounts of cell organelles would appear to be under separate control mechanisms.

- The inner mitochondrial membrane – under dual DNA control - continues to behave as an outlier.

DISCUSSION

Overview

The report focused on two sets of homogeneity postulates, the first well-established and the second an extension of the first. Both sets serve to define the relationship of structure to function in living organisms. By expressing this relationship mathematically (Equations 1 and 2), we begin the process of using the phenome – the downstream product of DNA – to predict and unravel upstream events.

The incentive for pursuing a general solution to the homogeneity postulates came from the finding of molecular biology that different species share remarkably similar or identical blueprints for many of their parts. From this it was reasoned that animal species must be subject to many – if not most - of the same rules.

Since we already know from earlier work with ratios that biology operates by rule (Bolender, 2011 to 2016), the problem became one of identifying a mathematical model capable of predicting events - consistent with a reality defined by biology. Given the understanding that prediction in biology requires equations with $R^2 = 1$ (Bolender, 2003) and given the model previously defined by deDuve's postulates, finding a solution consisted largely of reworking published data.

Postulates of deDuve

The **postulate of biochemical homogeneity** states that the members of a given population [in a cell] have the same biochemical composition. This means that a given amount of membrane surface area can be expected to define a given amount of marker enzyme activity. In effect, the postulate tacitly assumes a quantitative relationship between structure and function, as defined by Equations 1 and 2.

If we assume the postulates of deDuve's to be correct, then we would expect to find a table of equations with $R^2 = 1$ covering a wide range of cell organelles. Table 7 provides such a supporting document. Notice that these equations capture rules that biology has defined as ratios. Does this mean that biology encodes such rules in its DNA or do the rules come from recipes that biology can change as the need arises?

Table 7 Biochemical homogeneity allows us to predict enzymes from surfaces and surfaces from enzymes. In effect, relationships of structure to function become mathematically interchangeable. (Data adapted from Papers 1, 2, and 3).

INPUT X		PREDICT Y			
X	UNITS	Y	UNITS	EQUATION	R ² =
S(ER)	U/G	G-6-Pase	M ² /G	Y = 5.9625X	1
G-6-Pase	U/G	S(ER)	M ² /G	Y = 0.1677X	1
S(ER)	U/G	Esterase	M ² /G	Y = 46.657X	1
Esterase	U/G	S(ER)	M ² /G	Y = 0.0214X	1
S(ER)	U/G	NADPH-CCR	M ² /G	Y = 0.9829X	1
NADPH-CCR	U/G	S(ER)	M ² /G	Y = 1.0174X	1
S(OMIM)	U/G	MAO	M ² /G	Y = 0.6310X	1
MAO	U/G	S(OMIM)	M ² /G	Y = 1.5848X	1
S(IMIM)	U/G	CYOX	M ² /G	Y = 6.8150X	1
CYOX	U/G	S(IMIM)	M ² /G	Y = 0.1467X	1
S(PM)	U/G	S'NUC	M ² /G	Y = 26.267X	1
S'NUC	U/G	S(PM)	M ² /G	Y = 0.0381X	1

Why did it take so long to uncover the $R^2 = 1$ rules? By reporting research data as averages, we effectively forfeited the data of individual animals, which - as shown here - were needed to generate these equations (Table 1 vs. Table 2).

Reproducibility

Revisiting the homogeneity postulate would seem a timely exercise in view of the ongoing reproducibility crisis in biology (Baker, 2016). What needs to be done? Find out what's not working and then fix it. Let's look at a worked example to see how this approach can be applied to biochemistry.

Given the mathematical order assumed by the postulate of biochemical homogeneity, why can we predict enzyme activities from relative ratios (Table 4), but not from absolute values? This question became an issue when several published values were found to disagree with those of Amar-Costesec et al., 1974; Table II). Why did they disagree?

Consider this. If we relate enzyme activities to a mg of protein reference that varies from paper to paper, then this variation can be expected to affect the values reported for the enzymes. In effect, the mg protein reference represents a variable. What would happen, for example, if we standardized our assays - across publications - to the same amount of protein? Might disagreement suddenly become agreement? Given the plot shown in Figure 29, the answer appears to be yes. Now most of the biochemical results can be replicated.

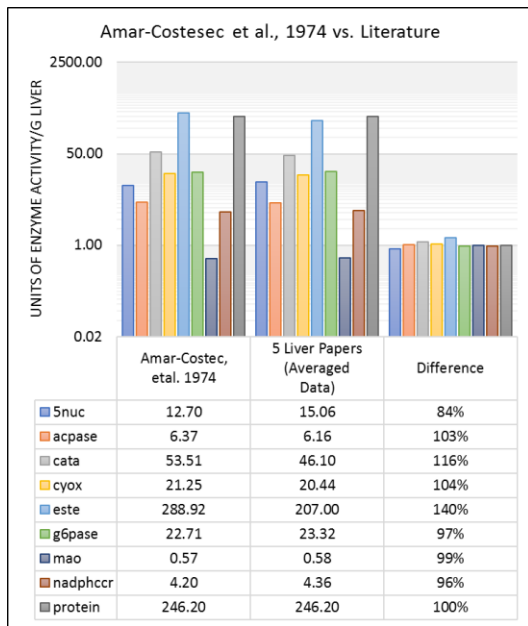


Figure 29 When enzyme assays are related to the same amount of protein, absolute values tend to come closer together.

Summary

- The relationship of structure to function exists as a biological rule (Equations 1 and 2), which can be captured with $R^2 = 1$ equations.
- Biology defines its precision and accuracy one organism at a time.
- Biochemical data can be standardized to a given amount of protein across publications.

Postulate of Biological Homogeneity

The **postulate of biological homogeneity** assumes that the same genetic information (DNA) produces the same parts within and across animals. In other words, $R^2 = 1$ equations derived from the cells of one species apply to all those species carrying the same DNA sequences.

Evidence in support of this new postulate came from deDuve's postulates, which were shown to apply repeatedly within a single species (Table

7) and often across multiple species (Figures 24-28).

Perhaps the strongest support for the postulate comes from Figure 26 (top panel). The patterns displayed by the hepatocytes of human and rat livers were clearly similar for five of the six organelle ratios.

Summary

- Equations 1 and 2 and strings of ratios can predict outcomes within and across animal species.
- When attempting to compare data collected from subjects under widely different conditions (e.g., age, sex, exposure, sampling, nutritional state), inconsistent results are to be expected.
- Using enzyme densities expressed as $R^2 = 1$ equations, both the structure and function of a cell can be reconstructed from a single data point with data coming from different species.

Enzyme Densities (ED)

Enzyme densities were used throughout the report to define relationships of structure to function, to detect patterns of biochemical homogeneity, and to predict data points. In effect, they are proving to be an effective data type for managing a wide range of complexities.

Enzyme densities offer the promise of moving events occurring in the phenome one step closer to their antecedents in the genome. Recall that DNA microarrays can tell us what RNAs are being expressed, but such RNAs are still many steps removed from their final products in the cell. This is where enzyme densities and stereology can play an important role by filling in the missing dots. Translating gene expression into changes expressed at the level of cellular membranes, for example, is

going to require detailed information about (1) changes in membrane surface areas, (2) changes in the packing densities of molecules in the membranes, and (3) changes in the rates of membrane turnover. Such information should prove invaluable as we begin to generate complexities parallel to the ones existing in the genome.

Equations 4, 5, and 6 and their method of solution might also be telling us something about the basic strategy of living systems. Since the simultaneous solution to pairs of linear equations is akin to linear programming, an enzyme density may represent an optimal solution to the problem packing enzymes in membranes, one that provides specific advantages to an organism. In effect, optimization may explain adaptability.

The biggest surprise, however, was how quickly enzyme densities and their $R^2 = 1$ equations triggered the transition to prediction. Starting with control data, we can now do all the following.

- Predict morphology from biochemistry.
- Predict biochemistry from morphology.
- Predict morphology from morphology.
- Predict biochemistry from biochemistry.

It will be interesting to see how long it takes to repeat these predictions in experimental settings when so many parts are changing at the same time.

First Principles (Rules)

To the list of rules started earlier (Bolender, 2016; Page 100), we can add four new ones.

Structure to Function Rule: Biology defines relationships of structure to function within tight tolerances, as shown by equations with $R^2 = 1$.

Prediction Rule: Prediction in biology requires data fitted to equations with $R^2 = 1$ or $R^2 \approx 1$.

Amounts Rule: Biology defines the relative amounts of its parts (e.g., molecules, organelles, cells, etcetera) with well-defined ratios, but allows their absolute amounts to vary markedly.

Mitochondrial Discontinuity Rule: Mitochondrial parts and their relationships of structure to function can be defined by genetic coding coming from both nuclear and mitochondrial DNA. Consequently, rules defined by nuclear DNA may not apply.

Bias, Contamination, and Average Data

When running - in parallel - morphological and biochemical experiments within the framework of analytical fraction, identifying sources of error (bias and contamination) and applying corrections was central to the experimental design of Papers 1 to 3.

Estimates for membrane surface areas, for example, carry biases determined by the sizes and shapes of the membranes relative to the section thickness. Moreover, the same membrane organelles come with one set of biases in the intact tissue, but the same membranes assume an entirely different set of biases in each of the five consecutive tissue fractions. This required the application of corrections for the section related biases prior to calculating the morphological recoveries (Paper 1).

The liver itself can become a major source of contamination in that it contains cells other than hepatocytes (e.g., endothelial, fat-storing, and Kupffer cells). Contributions from these contaminating cells can be avoided when estimating membrane surface areas in the

intact tissue by simply ignoring them, but this is not the case in the tissue fractions. As described in Papers 1, 2, and 3, the stereological estimates had to be corrected for both related biases and cell contaminations. Overestimates for membrane surface areas were corrected according to Weibel and Paumgartner (1978) and the extra-hepatocytic contaminations were accounted for using the data of Blouin et al., (1977).

Figures 30 and 31 tell the bias story most effectively. The uncorrected data of Figure 30 leads to failure ($R^2 \neq 1$ and the curve misses the origin), whereas the corrected data (Figure 31) leads to success (an equation with a $R^2 = 1$ that passes through the origin). Given the Weibel-Paumgartner corrections, we now have $R^2 = 1$ equations, an empirical proof for the postulates of deDuve, prediction, and a mathematical strategy for advancing toward the genome.

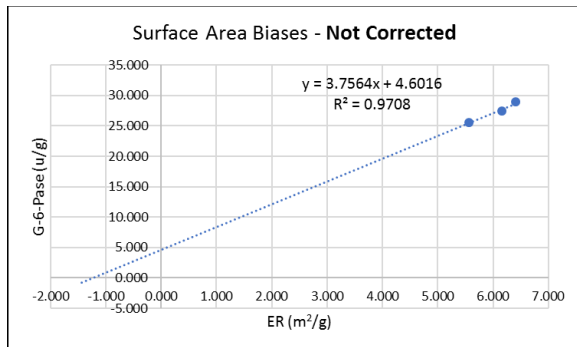


Figure 30 Stereological estimates for membrane surface areas – uncorrected for section related biases – produce unusable results. Compared to corrected data in Figure 31, the slopes differ by 59% (5.9625/3.7564).

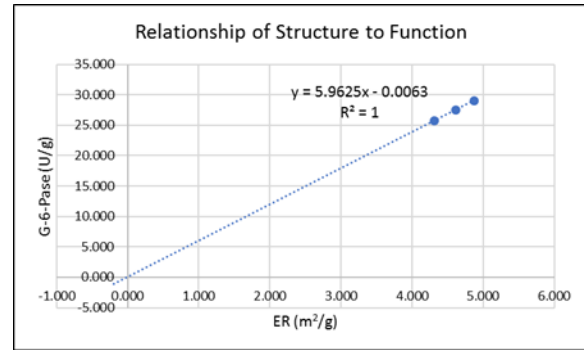


Figure 31 When corrected for biases according to Weibel and Paumgartner (1978), stereological data - in combination with biochemistry - provide ready access to otherwise undetectable relationships of structure to function in biology.

Although Figure 31 and several similar plots were needed to support the biochemical homogeneity postulate, we have yet to address the practical problem of having to deal largely with published data expressed as averages. What can we do? The simplest solution would be to plot enzyme densities (ED) as $R^2 = 1$ equations. If, for example, we average the data given in Table 4 and divide the average units of activity by the average surface area, we get an ED of 5.9611. When expressed as a structure-function equation, we have:

$$Y = 5.9611X \quad (5)$$

Notice that a plot of equation 5 (Figure 32) produces a curve that is almost identical to the one shown in Figure 31: $Y = 5.9611X$ vs. $Y = 5.9625X$. This option of being able to generate a $R^2 = 1$ equation from a single point (ED), will become invaluable as we continue to predict our way into biological complexity.

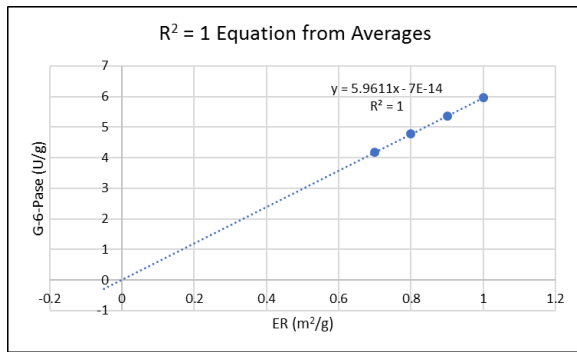


Figure 32 Given an enzyme density (ED), a $R^2 = 1$ curve passing through the origin can be readily generated.

Concluding Comments

In terms of the big picture, where are we?

Since DNA is linked to genes, genes to molecules, molecules to organelles, organelles to cells, and cells to organisms, we know that connectivity is fundamental to understanding biology. In solving the biology puzzle, we want to be able to connect its morphological and biochemical parts and then use relationships of structure to function to create pathways capable of shuttling information back and forth between DNA and its products distributed throughout all parts of the phenotype. This process is now underway.

What have we learned so far?

We know that we can use stereology to quantify morphology, biochemistry to quantify molecules, and published data to discover that biology uses ratios as its central organizing principle. By tapping into this principle, we can explore biology with patterns (mathematical markers, connection ratios), which, in turn, can direct us to biological rules – often expressed as $R^2 = 1$ equations. In turn, these equations, which bring diagnosis and prediction into the game, will play an essential role as we begin to explore the ways in which biology responds and adapts to adversity.

Why is this new approach to analyzing data immediately important to biology?

Since we have now begun the process of modifying our human genome with CRISPR, having a robust feedback loop from the phenotype – one based on empirical data and biological principles – becomes an essential ingredient for success and perhaps even for survival.

What type of game are we playing?

There are two types of games we can play with biology: zero-sum (win-lose) and nonzero-sum (win-win or lose-lose). Although the win-win option would appear to be the most promising, it is rarely used in biomedical research because the cost of entry is too high. It requires shifting to a theory structure consistent with biological complexity. By prototyping such a theory structure, the Enterprise Biology Software Project has been playing a non-zero-sum game (win-win) successfully for several years. Since biology already knows the answers to most of our questions, the strategy behind our game plan is quite simple. Whenever we construct a parallel complexity correctly, biology promptly answers our questions. In effect, we're using the parallel complexity as a communication device, wherein mathematics is the common language.

Prediction is the game changer...

REFERENCES

Alberts, B., Johnson, A., Lewis, J., Morgan, D., Raff, M., Roberts, K., Walter, P. *Molecular Biology of the Cell* 6th Edition 2014 Garland Science, New York; 1464 pages.

Amar-Costesec A., Beaufay H., Wibo M., Thinès-Sempoux D., Feytmans E., Robbi M., Berthet J. (1974) Analytical study of microsomes and isolated subcellular membranes from rat liver. II. Preparation and composition of the microsomal fraction. *J Cell Biol.* 61:201-212. (Free download).

Baker, M. (2016) Is There A Reproducibility Crisis? *Nature* 533, 452–454 (26 May 2016) doi:10.1038/533452a; Nature's Questionnaire (2016) : http://www.nature.com/polopoly_fs/7.36741%21/file/Reproducibility%20Questionnaire.doc

Beaufay, H., Amar-Costesec A., Thinès-Sempoux D., Wibo M., Robbi M., Berthet J. (1974) Analytical study of microsomes and isolated subcellular membranes from rat liver. III. Subfractionation of the microsomal fraction by isopycnic and differential fractionation in density gradients. *J Cell Biol.* 61:213-231.

Blouin A., Bolender R.P., Weibel E.R. (1977) Distribution of organelles and membranes between hepatocytes and nonhepatocytes in the rat liver parenchyma. A stereological study. *J Cell Biol.* 72(2):441–455.

Bolender, R. P. (1981) Stereology: Applications to pharmacology. *Ann. Rev. Pharmacol. Toxicol.* 21:549-573.

Bolender, R. P. 2003 *Enterprise Biology Software* IV. Research (2003) In: *Enterprise Biology Software*, Version 11.0 © 2003 Robert P. Bolender

Bolender, R. P. 2011 *Enterprise Biology Software* XII. Research (2011) In: *Enterprise Biology Software*, Version 11.0 © 2011 Robert P. Bolender

Bolender, R. P. 2012 *Enterprise Biology Software* XIII. Research (2012) In: *Enterprise Biology Software*, Version 12.0 © 2012 Robert P. Bolender

Bolender, R. P. 2013 *Enterprise Biology Software* XIV. Research (2013) In: *Enterprise Biology Software*, Version 13.0 © 2013 Robert P. Bolender

Bolender, R. P. 2014 *Enterprise Biology Software* XV. Research (2014) In: *Enterprise Biology Software*, Version 14.0 © 2014 Robert P. Bolender

Bolender, R. P. 2015 *Enterprise Biology Software* XVI. Research (2015) In: *Enterprise Biology Software*, Version 15.0 © 2015 Robert P. Bolender

Bolender, R. P. 2016 *Enterprise Biology Software* XVII. Research (2016) In: *Enterprise Biology Software*, Version 16.0 © 2015 Robert P. Bolender

Bolender, R.P. (2016) *Playing the Complexity Game with Biology*. © 2016 *Enterprise Biology Software Project*, PO Box 292 Medina, WA 98039-0292

Bolender R. P., Paumgartner D., Muellener D., Losa G., Weibel E. R. (1978) Integrated stereological and biochemical studies on hepatocytic membranes. I. Membrane recoveries in subcellular fractions. *J Cell Biol.* 1978 May 1; 77(2): 565–583. (Free download)

Bolender R. P., Paumgartner D., Muellener D., Losa G., Weibel E. R. (1980) Integrated stereological and biochemical studies on hepatocytic membranes. IV. Heterogeneous distribution of marker enzymes on endoplasmic

reticulum membranes in fractions J Cell Biol. Jun;85(3):577-86.

DeDuve, C. Principles of tissue fractionation. J Theor Biol. 1964 Jan;6(1):33–59.

deDuve, C. Exploring cells with a centrifuge. Nobel Lecture, December 12, 1974

de la Iglesia, F. A., Sturgess J. M., McGuire E. J., Feuer, G. (1976) Quantitative microscopic evaluation of the endoplasmic reticulum in developing human liver. Am J Pathol. Jan; 82(1): 61–70.

Hess F. A., Gnägi H. R., Weibel E.R., Preisig R. Morphometry of dog liver: comparison of wedge and needle biopsies. (1973) Virchows Arch B Cell Pathol 12: 303-317.

Holliday M. A., Potter, D., Jarrah, A, Bearg, S. (1967) The Relation of Metabolic Rate to Body Weight and Organ Size. Pediat. Res. 1: 185-195.

Koch M. M., Freddara U., Lorenzini I., Giampieri M. P., Jezequel A. M., Orlandi F. (1978) A stereological and biochemical study of the human liver in uncomplicated cholelithiasis. Digestion 18(3-4):162-177.

Lodish, H., Berk, A., Kaiser, C. A., Krieger, M., Bretscher, A., Ploegh, H., Amon, A., Martin, K. C. 2016 Molecular Cell Biology 8th Edition, W. H. Freeman, New York.; 1170 pages.

Losa G. A., Weibel E. R., Bolender R. P. (1978) Integrated stereological and biochemical studies on hepatocytic membranes. III. Relative surface of endoplasmic reticulum membranes in microsomal fractions estimated on freeze-fracture preparations. J Cell Biol. 1978 78: 289-308.

Roessner A., Kolde G., Stahl K., Blanke G., van Husen N., Themann H. (1978) Ultrastructural morphometric investigations on normal human liver biopsies. Acta Hepatogastroenterol (Stuttg) ;25(2):119-123.

Weibel E. R., Paumgartner D. (1978) Integrated stereological and biochemical studies on hepatocytic membranes. II. Correction of section thickness effect on volume and surface density estimates. J Cell Biol. 1978 77: 584-597.

Youfen Li, Jeong-Soon Park, Jian-Hong Deng, and Yidong Bai (2006) Cytochrome c oxidase subunit IV is essential for assembly and respiratory function of the enzyme complex. J Bioenerg Biomembr. J Bioenerg Biomembr. 2006 Dec; 38(5-6): 283–291.